

Influence of Non-glide Stresses on the Peierls Energy of Screw Dislocations

Keisuke KINOSHITA* Tomotsugu SHIMOKAWA
Toshiyasu KINARI Hideaki SAWADA
Kazuto KAWAKAMI Kohsaku USHIODA

Abstract

We investigate the influence of non-glide stresses on the Peierls energy of screw dislocation by using Nudged-Elastic-Band method. The influence of the applied non-glide stress fields on the Peierls energy of a screw dislocation is clearly observed. Moreover, we find that the stress field dependence of the Peierls energy is changed by the moving direction of the screw dislocation under a specific applied stress field. Geometrical parameters, which can measure the atomic elastic deformation around the screw dislocation core, are introduced to explain the stress field dependence of the Peierls energy. Finally, the cross slip of a screw dislocation around a precipitate with a misfit strain is discussed by combining the analytical solution of stress fields around the precipitate with the geometrical parameters obtained by our atomic simulations.

1. Introduction

Precipitation strengthening refers to a strengthening method for making strong metallic materials using precipitate in the parent phase as an obstacle to dislocation. At this time, dislocation can pass through the precipitate by sliding in the precipitate or by forming a dislocation loop around the precipitate. The former is the cutting mechanism and the latter is the Orowan mechanism.¹⁾ Which one of these mechanisms occurs is closely related to the resistance of the precipitate. On the other hand, before these mechanisms are completed, cross-slip may be generated from the dislocation line zone with a screw component to avoid the precipitate. It has been reported that the critical resolved shear stress (CRSS) at that time does not exceed half of that in the Orowan mechanism.²⁾ In other words, if the area around the precipitate is in the state that is likely to cause cross-slip, it means that the precipitation strengthening does not effectively function. Therefore, it is necessary to clarify the factors that may exert influence on the cross-slip of the screw dislocation.

Recently, it has been reported that if specific stress (referred to as non-glide stress in this study) that does not contribute to the Peach-Koehler (PK) force generated in a screw dislocation existing in the body centered cubic (bcc) metal is externally applied to the screw dislocation using the molecular dynamics simulation, the

screw dislocation moves on the slip plane that is different from the slip plane with the maximum resolved shear stress (RSS) but geometrically equivalent.^{3,4)} In order for the dislocation to make slip motion, it is necessary to overcome Peierls energy attributable to the periodic structure of the crystal.

In other words, the result of the above molecular dynamics calculation suggests that the Peierls energy of each geometrically equivalent slip system group is subject to different influence according to the stress field applied. Consequently, if the stress field is generated around a precipitate (for example, a coherent precipitate that causes misfit strain), the stress field increases (decreases) the Peierls energy of the slip system activated and decreases (increases) the Peierls energy of the other slip systems, the cross-slip of the screw dislocation adjacent to the precipitate may be accelerated (suppressed).

In this study, using the atomic simulation, non-glide stress is applied to the screw dislocation in α -Fe, and how the Peierls energy for the slip motion of the dislocation in the direction that is geometrically equivalent changes is investigated. Furthermore, using the results of the investigation, we consider the relationship that can be theoretically evaluated between the stress field around the coherent precipitate and the cross-slip of the screw dislocation. For the atom-

* Dr.Eng., Fundamental Metallurgy Research Lab., Advanced Technology Research Laboratories
1-8 Fuso-cho, Amagasaki, Hyogo Pref. 660-0891

ic simulation, open-sourced LAMMPS⁵⁾ is used and the stress field dependency of the Peierls energy is obtained by using the Nudged Elastic Band (NEB) method⁶⁾.

In this paper, Chapter 2 describes the analysis model and the inter-atomic potential energy. Chapter 3 describes the influence of the non-glide stress on the Peierls energy of the screw dislocation, and the validity of the results obtained is investigated under different periodic boundary conditions and the inter-atomic potential energy. In Chapter 4, why the Peierls energy is changed by the non-glide stress is considered by focusing on the change of the atomic structure near the dislocation core. In addition, how the stress field around the coherent precipitate exerts influence on the cross-slip of the screw dislocation is considered. Lastly, the conclusion of this paper is given in Chapter 5.

2. Analysis Model and Analysis Conditions

2.1 Analysis model

In this study, the analysis target is α -Fe. The crystal orientations in the directions of x , y and z are $[11\bar{2}]$, $[111]$ and $[1\bar{1}0]$, respectively. Here, the lattice constant of α -Fe is a_0 . Three vectors are defined as $\mathbf{v}_{[11\bar{2}]} = a_0[11\bar{2}]/3$, $\mathbf{v}_{[111]} = a_0[111]/2$ and $\mathbf{v}_{[1\bar{1}0]} = a_0[1\bar{1}0]$. Using these vectors, analysis zone \mathbf{e}_i^s , which has two different periodic boundary conditions is indicated as follows. First model \mathbf{e}_i^s is:

$$\mathbf{e}_1^s = 14\mathbf{v}_{[11\bar{2}]}, \mathbf{e}_2^s = 16\mathbf{v}_{[111]}, \mathbf{e}_3^s = 24\mathbf{v}_{[1\bar{1}0]} + \frac{1}{2}\mathbf{v}_{[111]} \quad (1)$$

In this study, this is called the square model. Second model \mathbf{e}_i^p is:

$$\mathbf{e}_1^p = 14\mathbf{v}_{[11\bar{2}]}, \mathbf{e}_2^p = 16\mathbf{v}_{[111]}, \mathbf{e}_3^p = 24\mathbf{v}_{[1\bar{1}0]} + 7\mathbf{v}_{[11\bar{2}]} + \frac{1}{2}\mathbf{v}_{[111]} \quad (2)$$

This is called the parallelogram model.

Figure 1(a)(b) shows the analysis zone of each model, indicating that the difference between these two analysis models is the periodic boundary condition in the z direction. For each model, a screw dislocation pair with a distance of 5 nm in between in the x direction is placed at the center. Figure 1(a)(b) shows the τ_{yz} stress field of each model including the screw dislocation pair. In this study, the screw dislocation on the left is referred to as S1 and the screw dislocation on the right is referred to as S2. Since the screw dislocation of S1 has the Burgers vector of $\mathbf{b}_{S1} = 1/2[111]$, the screw dislocation of S2 has the Burgers vector of $\mathbf{b}_{S2} = -\mathbf{b}_{S1}$. As described later, since this study focuses on the motion of easy-core screw dislocation, in this analysis model to which the periodic boundary conditions are applied, it is necessary to note that the distance in the x direction (distance between S1 and S2 and distance between S2 and S1') between adjacent screw dislocations is not strictly equal. (The

difference of the distances is smaller than a_0 .)

Each model uses different periodic boundary conditions in the z direction. As shown in Fig. 1(a), in the square model, the dislocations that have the same Burgers vector are periodically aligned in the z direction. In contrast, as shown in Fig. 1(b), in the parallelogram model, the screw dislocations that have different Burgers vector in the z direction are periodically aligned. The interaction between adjacent dislocations is different, and the different stress field in the analysis zone can be confirmed from Fig. 1(a)(b). Here, \mathbf{e}_3 is inclined in the y direction by $1/2\mathbf{v}_{[111]}$ for both models. This is equivalent to the plastic strain generated by putting the screw dislocation pair in the calculation cell. Considering this $1/2\mathbf{v}_{[111]}$ average stress τ_{yz} in the system can be made zero. Using the analysis model above, the influence of the non-glide stress on the Peierls energy of the screw dislocation is considered. In addition, by comparing the results obtained from two analysis models, the influence of the difference of the periodic structure of the screw dislocation is considered.

The screw dislocation core of bcc metal has energetically stable easy-cores and unstable hard-cores depending on its atomic geometry. Figure 1(c) shows the $\{111\}$ plane of the bcc structure. Here, the circles indicate atoms and the color difference indicates the depth difference in the $[111]$ direction. From this figure, it is confirmed that the $\{111\}$ plane has the three-layer periodic structure. In an easy-core, if displacement of the screw dislocation is superposed onto a bcc structure, each atomic configuration of the dislocation core maintains the three-layer structure that is the same as a perfect crystal. (The positions indicated by plotting squares in Fig. 1(c) correspond to easy-cores.) However, in a hard-core, atomic configurations of the dislocation core exist on the same $\{111\}$ plane. (In other words, atomic configuration of the dislocation core has the same color.) Therefore, the distance between adjacent atoms of a hard-core is shorter than that of an easy-core and the energy of dislocation becomes higher.⁷⁾ In this study, a transfer phenomenon of the screw dislocation that exists in an easy-core to another adjacent easy-core is considered.

2.2 Inter-atomic potential

Two inter-atomic potentials to indicate α -Fe as the inter-atomic interaction are used. One is the embedded atom method (EAM)⁸⁾ by Chamati, et al. and the other is the EAM potential by Mendelev, et al.⁹⁾ Mendelev, et al. have studied five types of potentials, from which a potential that best describes a defect structure in bcc iron is used as the other one. By comparing the influence of non-glide stress on the Peierls energy of the screw dislocation obtained from these two inter-atomic potentials, the validity of the result obtained

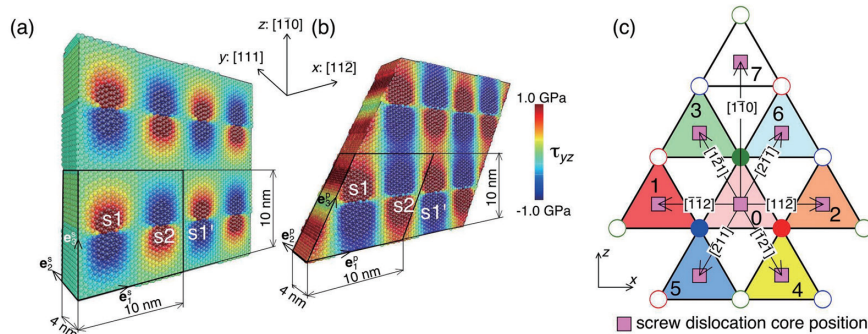


Fig. 1 Shear stress (τ_{yz}) field of analysis models expressed by Chamati potential with different periodic boundary conditions
(a) Square model, (b) Parallelogram model and (c) Atomic structure of $\{111\}$ planes in α -Fe and squares represent the position of easy-screw dislocation core.

is considered. The EAM potential by Chamati, et al. is developed to evaluate the surface diffusion and the EAM potential by Mendelev, et al. is developed to indicate the change of a phase from the liquid phase to the solid phase due to temperature change.

2.3 General description of the NEB method and analysis conditions

The NEB method is a technique to obtain the energy barrier necessary for transition from one state (an initial state) to another (a final state). Specifically, the atomic configurations of the initial and the final states are obtained first in some way and the atomic configurations during transition (these are referred to as images) are created by linear interpolation using the atomic configuration of the initial and the final state. Then, the linear spring is placed between their interpolated images. By relaxing the atomic configurations of each image while controlling the distances between each image, the minimum energy path in the transition phenomenon can be obtained.⁶⁾ In order to perform the NEB method, it is necessary to obtain atomic configurations of the initial and the final state. In this study, the difference of the atomic configurations between the initial and the final state are an easy-core position of the screw dislocations. The atomic configuration of the final state is that one of the screw dislocations is moved from the easy-core of the initial state to an adjacent easy-core position.

As the slip systems of bcc metal, two slip planes of the $\{112\}$ plane and $\{110\}$ plane are considered.¹⁰⁾ Now, we consider a case where the screw dislocation is at the position of “0” in Fig. 1(c). When moving on the $\{112\}$ plane, the dislocation core moves from “0” to “7” in the direction of $[1\bar{1}0]$. However, when the minimum energy path of this phenomenon is calculated using the NEB method, the movement from “0” to “7” is expressed by “0” \rightarrow “6” \rightarrow “7.” In other words, the phenomenon of the screw dislocation movement on the $\{112\}$ plane can be substituted with that in which the screw dislocation glides on two different $\{110\}$ planes. Therefore, in this study we examine the $\{110\}$ plane, i.e., the screw dislocation moving in the $\langle 112 \rangle$ direction.

The analysis models have a screw dislocation pair of S1 and S2. While S2 is fixed, S1 alone is allowed to move. At this time, the distance between the dislocations S1 and S2 is changed in accordance with the moving direction. The result obtained is considered to be influenced by the elastic interaction between the screw dislocations. Although $\langle 112 \rangle$ directions on the same $\{111\}$ plane have three directions, in this analysis, six directions are examined including the positive/negative moving directions (i.e., change of distance between S1 and S2).

Considering the above, the initial state and the final state used in this study are created as follows. First, a case where the dislocation core is present in the position of “0” shown in Fig. 1(c) is regarded as the initial state. A case where the dislocation core is present in the remaining positions from “1” to “6” is the state after the transition. For each analysis model, the stable structure on which each stress is loaded is obtained from the molecular dynamics simulation at the analysis temperature 0.1 K. The obtained stable structure is the initial coordinate and the final coordinate used in the NEB method. The external stress is considered to be uniaxial stress σ_x , σ_y , σ_z , or hydrostatic pressure $\sigma_{\text{hydro}} (= \sigma_x + \sigma_y + \sigma_z)$. When σ_{hydro} is applied, $\sigma_x = \sigma_y = \sigma_z$. The size of each external stress is -1.0, -0.5, 0, 0.5 and 1.0 GPa. These stresses are linearly applied from 0 MPa to the predetermined stress level in 50 000 steps (100 ps). Subsequently, the atomic configuration that is loaded with the predetermined stress is relaxed in the predetermined stress level in 100 ps at 0.1 K. It should

be noted that when a screw dislocation moves in any one of the directions “1”–“6” from “0,” these load stresses will become non-glide stresses that do not have influence on the PK force on the screw dislocations.

Using the obtained atomic configurations of the initial and the final states, 19 interpolation images are created. Then the influence of a non-glide stress on static Peierls energy of the screw dislocation is investigated using the NEB method. In this study, LAMMPS, which is an open source, is used to execute the normal NEB method for the first 10 000 steps. Then, the NEB method with climbing images⁶⁾ is performed until the maximum value of the force acting on the atoms is less than 0.001 eV/Å.

3. Analysis Result

3.1 Screw dislocation core structure

For bcc metal, two types of the screw dislocation core structure have been proposed to date, the non-degeneration type with a contracted core and degeneration type with a core expanding in three directions.¹¹⁾ As a result of the recent first-principles calculation, it is reported that the screw dislocation core of α -Fe becomes the three-fold symmetry non-degeneration type.^{12, 13)} In order to compare the screw dislocation core structure of the two interatomic potentials, the differential displacement (DD) vector is used.¹¹⁾ The DD vector is a method to indicate a dislocation core structure. To indicate a screw dislocation using the DD vector, a perfect crystal without the screw dislocation cores and atomic configurations with the screw dislocations are compared first to obtain atomic displacement u_y in the y direction. Then, for certain atom α , first neighbor atoms of α (that is β) on the $\{111\}$ plane are searched to obtain the size $|u_y^\alpha - u_y^\beta|$ of the displacement difference. The size of the DD vector shows the size of the displacement difference. The direction of the DD vector is the direction connecting the α atom and the β atom. The direction from an atom with small displacement to an atom with large displacement is regarded as a positive direction.

Figure 2(a)(b) shows each DD vector of the S1 screw dislocation after the load reduction indicated using the EAM potential by Chamati, et al. and the EAM potential by Mendelev, et al. Both of these dislocation cores are present in an easy-core. White circles represent atoms in the bcc structure, and the color difference represents the difference of the periodic atomic position in the y direction. In other words, atoms with the same color are present on the same xz plane. Solid circles in any colors represent defective atoms and these are non-bcc structure by the Common Neighbor Analysis method¹⁴⁾. It means that the center of the screw dislocation core is present in the triangle that consists of these defective atoms. Figure 2(a)(b) shows that the screw dislocation core structure is the three-fold symmetry non-degeneration type in the two inter-atomic potentials. As described previously, this result accords with the result of the first-principles calculation for α -Fe.

It is reported that if a non-glide stress exceeds a certain value, the DD vector of the screw dislocation is changed compared to a case without non-glide stress.^{3, 4)} Specifically, we discuss these results using coordinates of this study corresponding to the coordinates of the reported results. When $\sigma_x = -0.05c_{44}$ and $\sigma_z = 0.05c_{44}$ act at the same time on the analysis model with the screw dislocation, the DD vector expands in the directions of “3” to “6.” On the other hand, when $\sigma_x = 0.05c_{44}$ and $\sigma_z = -0.05c_{44}$ act at the same time, the DD vector expands in the directions of “1” and “2.” In contrast, under the conditions of the analysis in this study, a uniaxial stress, not a two-axial stress, is applied, and its absolute value does not exceed

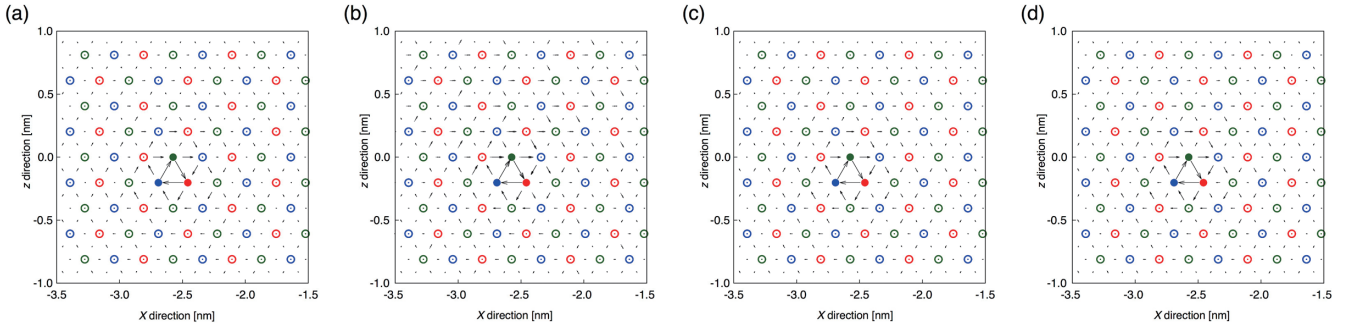


Fig. 2 Differential displacement vectors around a screw dislocation under no external loading expressed (a) Chamati potential, (b) Mendelev potential and under external loading, (c) $\sigma_x = -1.0$ GPa and (d) $\sigma_x = 1.0$ GPa expressed by Chamati potential. Open and closed circles represent atoms in the perfect bcc structure and in the screw dislocation core. Atomic colors represent the different depths of the stacking atomic layers along the [111] direction.

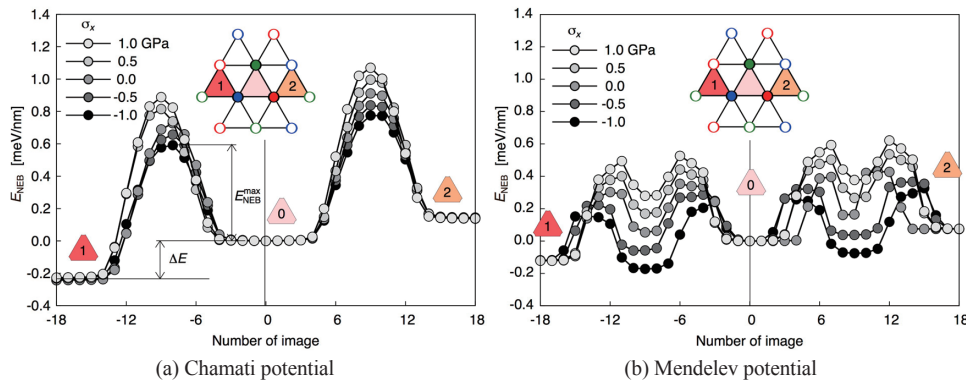


Fig. 3 Relationships between total energy E_{NEB} and image numbers of NEB analyses under external stress σ_x , screw dislocation core moves from “0” to “1” or “2”
Gray scale of circle plots represents values of σ_x .

$0.015c_{44}$. Therefore, as shown in Fig. 2(c)(d), if load stress $\sigma_x = \pm 1.0$ GPa is applied to the models with the screw dislocation using the EAM potential by Chamati, et al., the DD vector shows almost no change, but shows the three-fold symmetry structure of the non-degeneration type that is the same as Fig. 2(a). It has been confirmed that such tendency can be seen with non-glide stresses other than σ_x .

3.2 Non-glide stress dependency of Peierls energy

Figure 3(a)(b) shows energy change E_{NEB} of the entire system from the initial state when load stress σ_x is applied to the square models using the EAM potential by Chamati, et al. and the EAM potential by Mendelev, et al. and the screw dislocation moves from “0” to “1” or from “0” to “2”. The values on the horizontal axis are the image numbers interpolated by the NEB method. Image No. 0 has the screw dislocation core that is present at the position of “0” in Fig. 1(c). At image No. ± 18 , it has moved to the position of “1” or “2”. The contrasting density of the plot color represents the σ_x value.

For the EAM potential by Chamati, et al. in Fig. 3(a), it is confirmed that E_{NEB} shows a peak. For the EAM potential by Mendelev, et al. in Fig. 3(b), it is confirmed that E_{NEB} shows two peaks as reported by Gordon, et al.¹⁶⁾ According to the first-principles calculation¹²⁾ of the energy barrier for the screw dislocation movement by Itakura, et al., E_{NEB} shows one peak. Therefore, it is confirmed that the EAM potential by Chamati, et al. can reproduce the result of the first-principles calculation better than the EAM potential by Mendelev, et al.

However, these two interatomic potentials have a tendency in common in which the maximum value E_{NEB}^{\max} of E_{NEB} depends on non-

glide stress σ_x ; and in which the energy difference (ΔE) of the initial state and the final state does not depend on non-glide stress σ_x . These tendencies can be confirmed from other non-glide stresses. When the screw dislocation moves from 0 to 1, it is $\Delta E < 0$. When it moves from 0 to 2, $\Delta E > 0$. As described in 2.1 above, this is caused by the fact that the distances between adjacent dislocations are not equal. When the screw dislocation moves from 0 to 1, the minimum inter-dislocation distance is smaller than that when it moves from 0 to 2, which is considered one of the causes.

E_{NEB} obtained from the calculation in this study is the sum of the energy as follows. The first is energy E_σ attributable to plastic strain generated by the movement of the screw dislocation. The second is elastic interaction energy change $E_{int}^{(10)}$ due to the change of the screw dislocation pair distance. The last is Peierls energy E_p needed to move the dislocation to an adjacent easy-core.¹⁶⁾ If the values of E_σ and E_{int} are changed by a non-glide stress, ΔE should change. However, as shown in Fig. 3, ΔE shows the same value for each moving direction of the screw dislocations.

From these results, it is considered that the change of E_p due to the non-glide stress constitutes a large part of the cause of the non-glide stress dependency of E_{NEB}^{\max} calculated using the NEB method. In other words, the moving direction of the screw dislocation S1 can change the relative position to S2, but the influence of a non-glide stress on the Peierls energy of a screw dislocation can be evaluated using the non-glide stress dependency of E_{NEB}^{\max} obtained using the NEB method.

Figure 4 shows the dependency on each non-glide stress of E_{NEB}^{\max}

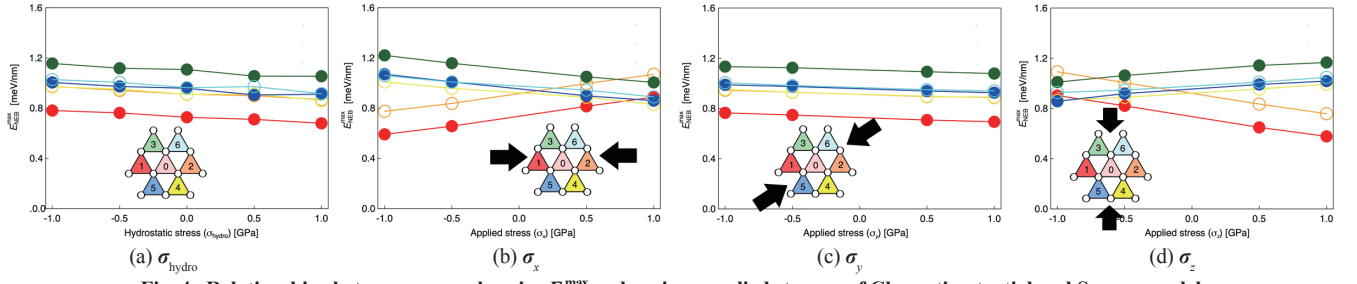


Fig. 4 Relationships between energy barrier $E_{\text{NEB}}^{\text{max}}$ and various applied stresses of Chamati potential and Square model
Colors of both circles and lines correspond to the screw dislocation propagation direction.

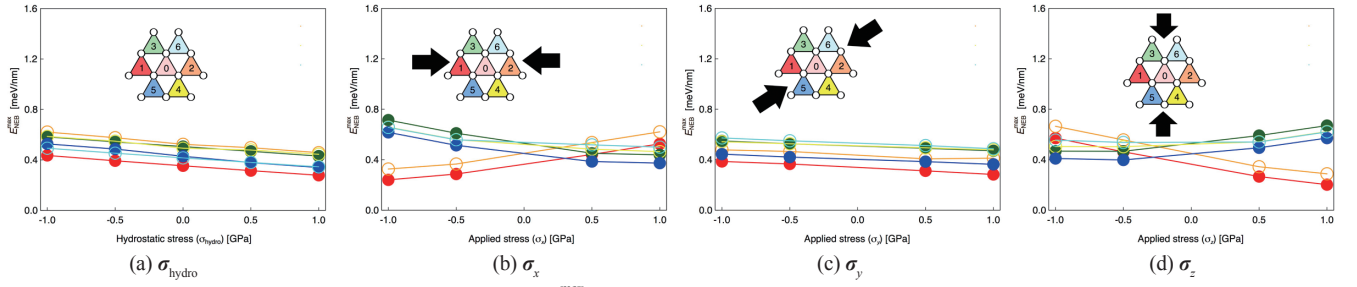


Fig. 5 Relationships between energy barrier $E_{\text{NEB}}^{\text{max}}$ and various applied stresses of Mendelev potential and Square model
Colors of both circles and lines correspond to the screw dislocation propagation direction.

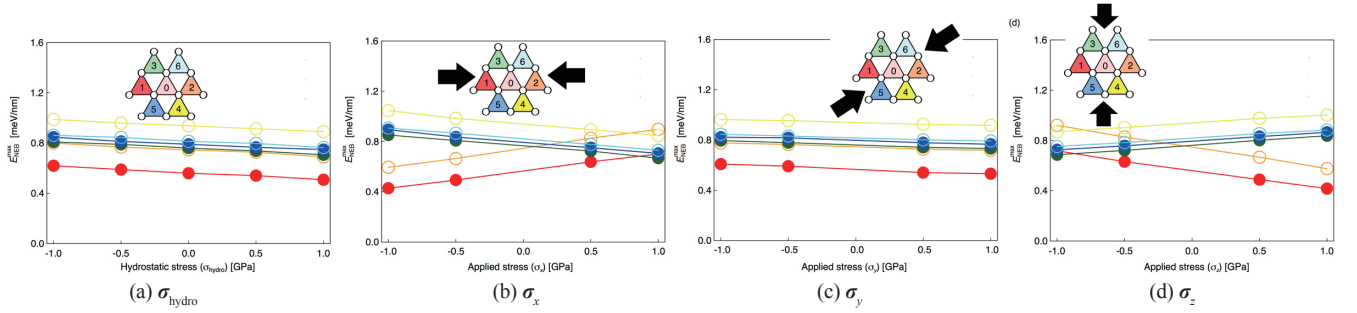


Fig. 6 Relationships between energy barrier $E_{\text{NEB}}^{\text{max}}$ and various applied stresses of Chamati potential and Parallelogram model
Colors of both circles and lines correspond to the screw dislocation propagation direction.

the square model using the EAM potential energy by Chamati, et al. As shown in Fig. 4(a), when σ_{hydro} is applied, $E_{\text{NEB}}^{\text{max}}$ becomes larger in the compression condition, not depending on the moving direction of the screw dislocation, whereas $E_{\text{NEB}}^{\text{max}}$ becomes smaller in the expansion condition. As shown in Fig. 4(c), when σ_y (normal stress of the dislocation line direction) is applied, the same trends are shown. From the relations of $E_{\text{NEB}}^{\text{max}}$ with non-glide stresses, σ_{hydro} or σ_y does not have influence on the moving direction of the screw dislocation.

Next, a case where σ_x or σ_z is applied perpendicular to the dislocation line is considered. At this time, the non-glide stress dependency of $E_{\text{NEB}}^{\text{max}}$ is influenced by the moving direction of the screw dislocation. As shown in Fig. 4(b), σ_x dependency of $E_{\text{NEB}}^{\text{max}}$ represents positive relations when moving in the directions toward “1” and “2”. When moving in the directions toward “3”–“6,” negative relations can be seen. On the other hand, as shown in Fig. 4(d), σ_z dependency of $E_{\text{NEB}}^{\text{max}}$ shows a tendency that is opposite to the case of σ_x .

Figures 5 and 6 show the non-glide stress dependency of $E_{\text{NEB}}^{\text{max}}$ the square model using the EAM potential by Mendelev, et al. and of the parallelogram model using the EAM potential by Chamati, et al. When compared to Fig. 4, while the absolute value of $E_{\text{NEB}}^{\text{max}}$ is different, all of the non-glide stress dependencies of $E_{\text{NEB}}^{\text{max}}$ show the

same tendency, not influenced by the periodic structure of the screw dislocation or the interatomic potentials used.

Summarizing the results above, first it was found that the Peierls energy of a screw dislocation was changed by the non-glide stress that does not exert influence on the PK force of the dislocation. Next, it was found that the non-glide stress dependency of Peierls energy was changed by a non-glide stress component and also influenced by the moving direction of the dislocation. Lastly, it was confirmed that the tendency of the Peierls energy's non-glide stress dependency did not depend on the periodic structure of the screw dislocation or the inter-atomic potentials used. The results obtained here show a favorable correspondence relationship with the conditions for the transition of the slip system of a screw dislocation as reported by Gröger, et al. who also used the molecular dynamics simulation.⁴⁾

4. Discussion

4.1 Relationship between crystal structure change and Peierls barrier

The result of this study confirmed that the Peierls energy of the screw dislocation was changed by a non-glide stress that does not

exert influence on the PK force of the dislocation. In addition, in view of the fact that the non-glide stress dependency of the Peierls energy is influenced by the moving direction of the dislocation, in order to understand the mechanism, more detailed study is required. Here, focusing on the change of the atomic configuration around the dislocation core by a non-glide stress, the reason why Peierls energy shows the dependency on a non-glide stress is considered. For this purpose, two parameters indicating the change of the atom structure as described below are introduced. The first one focuses on the atomic configuration of a plane perpendicular to the dislocation line ($\{111\}$ plane). The deformation of the triangular grid (the direction of each side is $[11\bar{2}]$, $[1\bar{2}1]$ and $[2\bar{1}1]$. Refer to Fig. 1(c).) that constitutes the plane which is indicated as follows:

$$P_A = \frac{A_s - A_{s0}}{A_{s0}} \quad (3)$$

where A_s is the aspect ratio obtained by dividing the triangle height by the length of the base that is in the screw dislocation moving direction for the triangular grid that constitutes the $\{111\}$ plane, and A_{s0} is the aspect ratio ($=\sqrt{3}/2$) of a regular triangle. Therefore, P_A is a parameter that indicates the distortion of the triangle that constitutes a plane perpendicular to the dislocation line due to a non-glide stress. If it is positive, the height of the triangle is longer than a regular triangle, while if it is negative, the shape of the triangle is one horizontally longer than a regular triangle. For the second parameter, the changing ratio of the distance between $\{111\}$ planes is indicated as follows:

$$P_L = \frac{L - L_0}{L_0} \quad (4)$$

L represents the distance between the $\{111\}$ plane in each model and L_0 represents L without applied stress. In other words, P_L is a parameter that indicates the length change of the dislocation line by a non-glide stress. A positive value indicates positive strain that occurs in the direction of the screw dislocation line, which means that the dislocation line extends. In contrast, a negative value indicates negative strain that occurs in the direction of the screw dislocation line, meaning that the dislocation line is shortened.

Figure 7 shows the change of $E_{\text{NEB}}^{\text{max}}$ for P_A and P_L (square model, interatomic potential energy is Chamati et al.). Looking at Fig. 7(a), the change of P_A by σ_x or σ_z is larger than σ_{hydro} or σ_y . On the other hand, looking at Fig. 7(b), the change of P_L by σ_{hydro} or σ_y is larger than σ_x or σ_z . If the change of P_A or P_L is large, $E_{\text{NEB}}^{\text{max}}$ shows a negative relationship. However, big changes of $E_{\text{NEB}}^{\text{max}}$ exist in each small change of P_A or P_L . For this reason, only P_A or P_L cannot uniformly describe the influence of all non-glide stress components on $E_{\text{NEB}}^{\text{max}}$.

Considering the sum of the two parameters above as P ($=P_A + P_L$), the relations with the Peierls energy are examined. **Figure 8(a)** shows the change of $E_{\text{NEB}}^{\text{max}}$ by P for the square model of the EAM potential by Chamati, et al.; Fig. 8(b) shows the change of $E_{\text{NEB}}^{\text{max}}$ by P for the square model of the EAM potential by Mendelev, et al.; and Fig. 8(c) shows the change of $E_{\text{NEB}}^{\text{max}}$ by P for the parallelogram model of the EAM potential by Chamati, et al. It is confirmed that $E_{\text{NEB}}^{\text{max}}$ in all models shows a negative correlation with P . Accordingly, the non-glide stress dependency of the Peierls energy can be

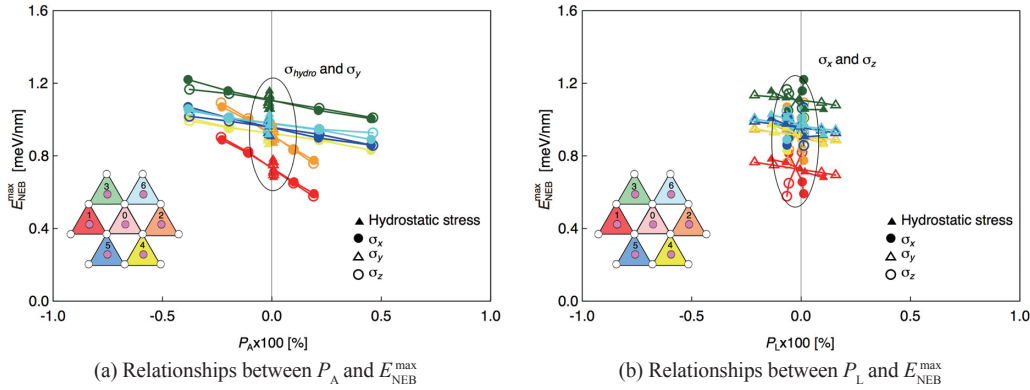


Fig. 7 Relationships between the geometrical parameter P_A or P_L and energy barrier $E_{\text{NEB}}^{\text{max}}$ of Chamati potential and Square model
 Colors of both marks and lines correspond to the screw dislocation propagation direction, Closed triangles: hydrostatic stress, Closed circles: σ_x , Open triangles: σ_y , Open circles: σ_z .

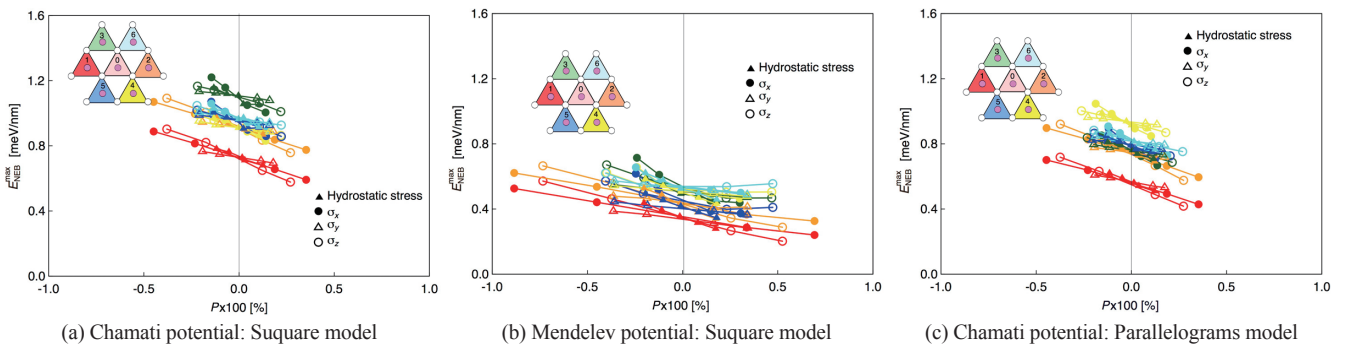


Fig. 8 Relationships between the geometrical parameter $P = P_A + P_L$ and energy barrier $E_{\text{NEB}}^{\text{max}}$
 Colors of both marks and lines correspond to the screw dislocation propagation direction, Closed triangles: hydrostatic stress, Closed circles: σ_x , Open triangles: σ_y , Open circles: σ_z .

understood by P .

In other words, due to the applied non-glide stress, when the screw dislocation moving distance is shorter than distances in two other equivalent directions, or when the dislocation line is extended, the Peierls energy of the screw dislocation becomes smaller. In contrast, when the moving distance is longer than those in other equivalent directions, or when the dislocation line is shortened, the Peierls energy of the screw dislocation is large. In addition, it is shown that the influence of P_A and P_L on E_{NEB}^{\max} is approximately one-to-one correspondence. Now, focusing on the fact that the change in the crystal structure described by P does not influence the PK force, which is involved in the motion of the screw dislocation, it is clear that the Peierls energy of the screw dislocation motion in bcc metal is changed not only by shear stress involved in the PK force as indicated by Gordon, et al.,¹⁵⁾ and but also by the deformation of the crystal structure attributable to the non-glide stress.

Furthermore, when the EAM potential by Mendelev, et al. is used, it is confirmed that the value range of P is larger than others. We think this is because c_{11} of the EAM potential by Mendelev, et al. is larger by 0.9% than the EAM potential by Chamati et al., whereas c_{12} is smaller by 1.2%, the potential energy of the EAM potential by Mendelev, et al. causes the change of the atom structure by the non-glide stress to become larger than the EAM potential by Chamati et al.

4.2 Relationship between the stress field of coherent spherical precipitate and cross-slip

In this section, using the results described above, interaction of the coherent spherical precipitate and the screw dislocation is considered. If misfit strain $\bar{\epsilon}$ exists between the base metal and a precipitate, a stress field is generated around the precipitate. How the stress field exerts influence on the cross-slip of the screw dislocation is examined using geometric parameter P as introduced above.

Figure 9(a) shows the relations between the coordinate system considered here and the spherical precipitate using the position of the precipitate as the origin. Assuming that the screw dislocation of which the dislocation line extends in the y direction moves in a direction from the positive to negative on plane xy with $z > 0$, along the x direction, with a part of the dislocation line close to the precipitate. In this study, it is also assumed that the first cross-slip occurs on a plane of $y=0$ as a result of the influence of the precipitate stress field.

The stress field around the spherical precipitate coherently precipitated with misfit strain $\bar{\epsilon} \neq 0$ is indicated by the formula as follows in the linear elastic theory.¹⁷⁾

$$\sigma_{ij} = \frac{2\mu_M \bar{\epsilon} R^3}{r^5} \begin{bmatrix} r^2 - 3x^2 & 3xy & 3xz \\ 3xy & r^2 - 3y^2 & 3yz \\ 3xz & 3yz & r^2 - 3z^2 \end{bmatrix} \quad (5)$$

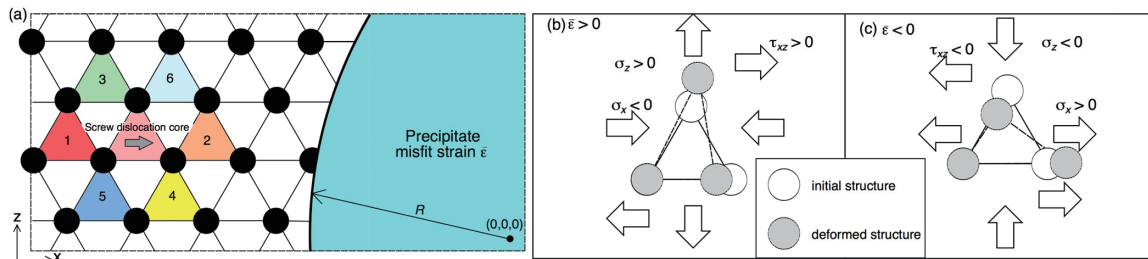


Fig. 9 (a) Schematic figure of interaction between a spherical precipitate and a screw dislocation, atomic structural change around the spherical precipitate with (b) $\bar{\epsilon} > 0$ and (c) $\bar{\epsilon} < 0$

where, $\bar{\epsilon}$ is misfit strain, R is radius of the spherical precipitate, and r is the distance from the origin ($=\sqrt{x^2+y^2+z^2}$). The stress component (τ_{xy} , τ_{xz}) involved in the PK force of the screw dislocation is ignored. Also, as σ_y has a certain level of influence on the screw dislocation motion in any direction according to the results of this study (Fig. 4(c), etc.), it is not considered in this study. From the stress components σ_x , σ_z and τ_{xz} obtained from the formula above, the change of the atomic configurations on plane (111) (xz plane) is considered in order to estimate P . Then, the relationships between the possibilities of the cross-slip occurring around the precipitates and $\bar{\epsilon}$ are considered. In other words, attention should be paid to the change of the triangle strain indicated by P_A .

First, the positive misfit strain of $\bar{\epsilon} > 0$ is considered. Considering that the slip plane of the screw dislocation approaching the precipitate is in the $1/\sqrt{3}$ range ($0 < z < R/\sqrt{3}$) of the precipitate radius from the plane passing through the center of the precipitate, the range on the plane of $y=0$ is always in the stress fields of $\sigma_x < 0$, $\sigma_z > 0$ and $\tau_{xz} > 0$. Also considering the signs of these stress components, the atomic configuration near the precipitate is changed in the shape as shown in Fig. 9(b). Now, P for each moving direction of “0” → “2” (the non-cross-slip direction), “0” → “4” and “0” → “6” (the cross-slip directions) of the screw dislocation is considered. First, according to Fig. 9(b), when the screw dislocation moves from “0” to “2,” P is larger than 0. This result means that the Peierls energy will be decreased.

When the screw dislocation moves “0” → “4” or “0” → “6,” P is smaller than 0. This result leads to the estimation that the Peierls energy will be increased. In other words, when $\bar{\epsilon} > 0$, the Peierls energy of the screw dislocation becomes smaller when the screw dislocation moves on the same slip plane (cross-slip does not occur) than when the screw dislocation moves on the other slip plane (cross-slip occurs). This result suggests that it is unlikely cross-slip occurs. On the other hand, when $\bar{\epsilon} < 0$, the stress field is always $\sigma_x > 0$, $\sigma_z < 0$ and $\tau_{xz} < 0$ in the same region as above, and the atomic configurations are changed to that as shown in Fig. 9(c). Therefore, when the screw dislocation moves from “0” to “6,” then P is larger than 0. This result leads to the estimation that the stress field is likely to generate cross-slip.

From the consideration above, it is confirmed that the stress field near the precipitate has influence that changes the Peierls energy of each slip system of the screw dislocation. Additionally, this result suggests that the misfit strain of the precipitate influences the cross-slip of screw dislocation. Therefore, although this consideration is limited to normal certain planes in the moving direction of the dislocation, the result described in this paper is expected to constitute useful guidelines for the strengthening design of metallic materials.

5. Summary

In this study, the influence of a non-glide stress that does not contribute to the dislocation motion with the Peierls energy of the screw dislocation in α -Fe was considered using the Nudged Elastic Band method. We note that the stress components applied to evaluate Peierls energy in this study do not influence the Peach-Koehler (PK) force acting on the screw dislocation. The results obtained in this study are as follows.

- The Peierls energy of the screw dislocation was changed by a non-glide stress that does not contribute to the dislocation motion, and this tendency was influenced by a non-glide stress component.
- The relationships between the Peierls energy and non-glide stresses did not depend on the periodicity position of the screw dislocation and the interatomic potentials.
- The relationships could be explained by using the change of the atomic configurations around the screw dislocation core.
- As a result of the consideration regarding the interaction between the screw dislocation and the precipitate using the results obtained in this study, we found the possibility of influence of the stress field around the precipitate on the cross-slip phenomenon.

Acknowledgment

This paper is a reproduction of that published in the Transactions of the Japan Society of Mechanical Engineers.¹⁸⁾ We express our

gratitude to the Japan Society of Mechanical Engineers who gave permission for reproduction.

References

- 1) Ardell, A.J.: Metallurgical and Materials Transactions A. 16 (12), 2131–2165 (1985)
- 2) Arzt, E., Ashby, M.F.: Scripta Metallurgica. 16 (11), 1285–1290 (1982)
- 3) Ito, K., Vitek, V.: Philosophical Magazine A. 81 (5), 1387–1407 (2001)
- 4) Gröger, R. et al.: Acta Materialia. 56 (19), 5401–5411 (2008)
- 5) Plimpton, S.: Journal of Computational Physics. 117, 1–19 (1995)
- 6) Henkelman, G. et al.: The Journal of Chemical Physics. 113 (22), 9901–9904 (2000)
- 7) Suzuki, H.: Dislocation Dynamics. New York, McGraw-Hill, 1968, p.679
- 8) Chamati, H. et al.: Surface Science. 600 (9), 1793–1803 (2006)
- 9) Mendelev, M.I. et al.: Philosophical Magazine. 83 (35), 3977–3994 (2003)
- 10) Hirth, J.P., Lothe, J.: Theory of Dislocations. John Wiley and Sons, 1982
- 11) Vitek, V., Perrin, R.C., Bowen, D.K.: Philosophical Magazine. 21 (173), 1049–1073 (1970)
- 12) Itakura, M. et al.: Acta Materialia. 60 (9), 3698–3710 (2012)
- 13) Frederiksen, S.L., Jacobsen, K.W.: Philosophical Magazine. 83 (3), 365–375 (2003)
- 14) Honeycutt, J.D., Andersen, H.C.: Journal of Physical Chemistry. 91 (19), 4950–4963 (1987)
- 15) Gordon, P.A. et al.: Modelling and Simulation in Materials Science and Engineering. 18 (8), 085008 (2010)
- 16) Hull, D., Bacon, D.J.: Introduction to Dislocations. 5th Edition. Elsevier Science, 2011, p.146
- 17) Eshelby, J.D. et al.: Solid State Physics. Vol. 3. New York, Academic Press, 1956
- 18) Kinoshita, K. et al.: Transactions of the JSME, 80 (809), CM0018 (2014)



Keisuke KINOSHITA
Dr.Eng.
Fundamental Metallurgy Research Lab.
Advanced Technology Research Laboratories
1-8 Fuso-cho, Amagasaki, Hyogo Pref. 660-0891



Tomotsugu SHIMOKAWA
Professor, Dr.Eng.
College of Science and Engineering
Kanazawa University



Toshiyasu KINARI
Professor, Dr.Eng.
College of Science and Engineering
Kanazawa University



Hideaki SAWADA
Senior Researcher, Dr.Eng.
Mathematical Science & Technology Research Lab.
Advanced Technology Research Laboratories



Kazuto KAWAKAMI
Senior Researcher, Dr.Eng.
Mathematical Science & Technology Research Lab.
Advanced Technology Research Laboratories



Kohsaku USHIODA
Executive Advisor, Dr.Eng.
Technical Research & Development Bureau